NMR in $CeAl_2$. Hyperfine fields, fluctuation rates, and spatial correlation in an unstable-moment system

D. E. MacLaughlin, O. Peña, and M. Lysak
Department of Physics, University of California, Riverside, California 92521
(Received 23 June 1980)

^{27}Al nuclear magnetic resonance (NMR) and nuclear quadrupole resonance (NQR) measurements in the antiferromagnetic and paramagnetic states of the intermetallic compound $CeAl_2$ have yielded information on the competition between magnetic ordering and moment instability in this system. In the antiferromagnetic state below $T_N = 3.9$ K the zero-field NQR linewidth increases from 12(2) kHz above T_N to 90(10) kHz at 1.5 K $= 0.4T_N$. This increase is consistent with the onset of a distribution of hyperfine fields in the spatially modulated antiferromagnetic structure suggested on the basis of neutron scattering studies, but the width of the hyperfine field distribution is more than a factor of 10 smaller than consistent with either the "single-q" modulated structure of Barbara and co-workers or low-temperature nuclear hyperfine specific-heat measurements. It is suggested that the large fraction of nuclei in small hyperfine fields is a consequence of moment modulation in more than one direction. Observed ^{27}Al spin-lattice relaxation rates below $\sim 0.65T_N$ were spatially distributed in the specimen: both "hard," magnonlike fluctuation modes and "soft" fluctuations, presumably associated with Kondo-like states in nodes of the modulated structure, were observed. The activation energy of 0.87(8) meV for the magnonlike modes is in good agreement with neutron results. In the paramagnetic state the ratio of the NMR shift to the bulk susceptibility varies with temperature in a way which is consistent with a simple model of anisotropic hyperfine coupling to the crystal-field-split Ce ionic states. The spin-lattice relaxation behavior above T_N indicates the onset of spatial short-range order at temperatures below ~ 100 K, but the nature of this order is uncertain due to difficulties in reconciling the NMR and neutron scattering data. If such short-range order is assumed to be absent at 300 K, comparison of NMR and neutron results indicates that effectively ~ 10 Ce neighbors are hyperfine coupled to a given ^{27}Al nucleus.

I. INTRODUCTION

The unstable $4f$ shell in alloys and intermetallic compounds containing cerium leads to a wide variety of interesting phenomena. These include the Kondo effect in dilute alloys,[1] related behavior in intermetallic compounds, configuration mixing or intermediate valence,[2] and competition between moment instability and magnetic ordering.[2,3] The compound $CeAl_2$ appears to exhibit a number of these phenomena. Numerous investigations of this system have indicated the presence of a complicated interplay between Kondo-like moment compensation, magnetic interactions between Ce ions, and the presence of a crystalline electric field (CEF) splitting.[4,5] The ^{27}Al nuclear resonance experiments reported in this paper have yielded information on transferred hyperfine mechanisms and hyperfine field distributions in $CeAl_2$, particularly in the modulated antiferromagnetic (AF) state below $T_N = 3.9$ K, and also on the relative roles played by spin-spin coupling and Kondo-like behavior in determining the dynamic fluctuation spectra.

$CeAl_2$ was first characterized as a "Kondo compound" on the basis of resistivity measurements,[4] which showed the minimum characteristic of the Kondo effect. In addition the existence of a CEF splitting $\Delta/k_B \sim 100$ K was inferred from thermodynamic and transport measurements,[5] but the least ambiguous determination of Δ and the CEF-split states was obtained from inelastic neutron scattering.[6] These and other studies[7] indicated also that the lifetime of Ce spin states was severely limited, presumably by a combination of Kondo-like fluctuations and spin-spin coupling between Ce ions.

The neutron magnetic Bragg scattering experiments of Barbara *et al.*[8] resolved previous uncertainty[2] concerning the ground state of $CeAl_2$ by demonstrating that the phase transition at 3.9 K signaled the onset of an AF low-temperature phase. The observed Bragg reflections could, however, only be understood by assuming spatial modulation of the Ce moment magnitude. The thermodynamics of this transition have been extensively investigated: the phase boundary in the magnetic-field–temperature plane has

been determined[2,9] and anisotropies, critical properties, etc., have been studied. The case for an AF ground state was strengthened by the observation[6] of magnonlike excitations below T_N in neutron scattering.

Recent neutron studies by Shapiro *et al.*[10] have concluded that the single direction of moment modulation originally proposed[8] is inadequate to explain all observed Bragg reflections. A "multiple-q" structure was suggested, with concurrent modulation in several crystalline directions.

Our results in the AF state are discussed in Sec. IV, and may be summarized as follows. Both ^{27}Al NMR and nuclear quadrupole resonance (NQR) yield a considerable fraction of the nuclei in regions of low Ce spin polarization. This is qualitatively consistent with Ce moment modulation; in addition, the NMR and NQR data suggest that the "multiple-q" structure is more appropriate than the "single-q" structure. Nuclear spin-lattice relaxation experiments in the AF state yield thermally-activated relaxation rate behavior, with an activation energy in good agreement with neutron data.[6] Additional relaxation at temperatures below $\sim 0.6 T_N$ suggests the presence of low-frequency Ce spin modes, which are possibly associated with Kondo-like spin fluctuations.[11]

Section V treats measurements in the paramagnetic (PM) state. Here an appreciable temperature variation of the average hf field was observed, as expected if the hf coupling to the Γ_7 doublet CEF ground state is different than that to the Γ_8 quartet excited state, due to anisotropy in the hf coupling strength.[12] PM-state spin-lattice relaxation measurements above ~ 200 K, together with quasielastic neutron-scattering linewidths,[13] yield an estimate of about 10 for the effective number of Ce neighbor ions coupled to a given ^{27}Al nucleus.[14] At lower temperatures, the situation regarding short-range Ce-Ce correlations in the PM state is ambiguous. No direct NMR evidence was found for Ce moment instability or Kondo compensation[11] in the PM state, or for crystal-field effects of the kind treated by Sugawara.[15]

Experimental techniques and results are discussed in Secs. II and III, respectively, and Sec. VI summarizes our conclusions. Preliminary reports of parts of this work have appeared previously.[16,17]

II. EXPERIMENTAL TECHNIQUES

Specimens of $CeAl_2$ were prepared by arc melting stoichiometric quantities of the elements Ce ($3N-4N$ pure) and Al ($6N$ pure). The ingots were turned and remelted several times to improve homogeneity, and after arc melting were either submitted to a homogenizing anneal of 800 °C for 2 days or left in the as-cast condition. Samples were prepared by crushing and sieving to various powder grain sizes between 45 and 90 μm. The NMR and NQR results were independent of heat treatment and particle size. Debye-Scherrer powder-pattern x-ray measurements gave no indication of second phases. The measured susceptibility agreed with previous results[18] to within experimental error over the temperature range 4.2–300 K.

NMR measurements were carried out in external fields between 4 and 12 kOe using a field-swept pulsed NMR apparatus and a continuous-wave (cw) Varian wide-line NMR spectrometer. NMR spectra (absorption versus field strength) were obtained with both units. The integrated pulsed spin-echo signal amplitude was averaged using a Nicolet 1170 signal enhancer, followed by data transfer to a Tektronix 4051 computer for analysis. The centroid of the second-order quadrupole-split $\frac{1}{2} \leftrightarrow -\frac{1}{2}$ transition was obtained numerically, and the paramagnetic shift was computed after correction for the quadrupolar contribution.[19] The cw spectrometer employed conventional lock-in detection. Extrema of the derivative spectra were used to obtain the isotropic and anisotropic shifts, K_i and K_a, respectively, as well as the quadrupole coupling constant e^2qQ/h, using techniques reported previously.[16] Relaxation measurements were carried out using standard spin-echo detection of the nuclear magnetization recovery after a train of saturating pulses.[19]

The susceptibility of paramagnetic $CeAl_2$ is high at low temperatures, and can result in appreciable corrections to the paramagnetic shift due to demagnetizing effects.[19] The Lorentz and demagnetizing fields give a temperature-independent contribution

$$H_{\rm dem} = (4\pi/3 - D) n \mu_B \tag{1}$$

to the field at the nuclei, where D is the sample demagnetization factor, $n = 1.53 \times 10^{22}$ cm^{-3} is the Ce number density, and μ_B is the Bohr magneton. Evaluation of D in our powdered samples is difficult, but the effect is probably small: $n\mu_B = 141$ Oe, which is only a few percent of the observed hyperfine field, and the factor $4\pi/3 - D$ should be of the order of unity.

Zero-field NQR measurements employed the ^{27}Al $\pm\frac{5}{2} \leftrightarrow \pm\frac{3}{2}$ transition at approximately 1.45 MHz.[20] The NQR technique was used for several reasons. First, it permits fairly direct determination of the distribution of magnetic hf fields in the AF state, without convolution with other magnetic and quadrupolar broadening mechanisms present in high-field NMR. Second, the absence of an applied permits study of an unperturbed AF state. Third, the NQR technique simplifies the interpretation of nonexponential relaxation recovery functions, as discussed below. Most relaxation data were taken using NQR; NMR measurements confirmed the NQR results at a few temperatures. Pulsed NQR spectroscopy was carried out by increasing spectrometer

bandwidth as much as possible and sweeping the frequency. In the AF state the resonance became so broad that the maximum obtainable bandwidth (~300 kHz) was still narrow enough to distort the lineshape appreciably. Attempts to use a marginal-oscillator NQR detector at this low frequency were unsuccessful.

In the presence of unequal nuclear spin-level splittings, spin-lattice relaxation recovery functions are nonexponential in general. This phenomenon has been discussed for quadrupole-split NMR by Narath[21] and for zero-field NQR by MacLaughlin *et al.*[22] The general solution to the master relaxation equation in these cases is a sum of exponential terms, with rate constants which are multiples of the rate $1/T_1$ which would have been obtained in the case of a pure Zeeman splitting. The coefficients of $1/T_1$ in the exponential terms are functions only of the nuclear spin, whereas the preexponential factors also depend on the initial saturation conditions.[21,22] These were not well known *a priori,* and were treated as free parameters in least-squares fits to data. The number of exponential terms for nuclear spin $I = \frac{5}{2}$ (^{27}Al) is two for NQR[22] and five for NMR.[21] It was thus felt that least-squares fits to NQR data would be more reliable, despite the reduction in signal-to-noise ratio at the lower resonance frequency, since fewer free parameters would be required for the fit.

III. EXPERIMENTAL RESULTS

A. Antiferromagnetic state

As discussed above, NQR was used for the most part to study nuclear resonance properties below the Néel temperature. Figure 1 gives the half-width half-maximum linewidth $\Delta\nu$ of the ^{27}Al $\pm\frac{5}{2} \leftrightarrow \pm\frac{3}{2}$ NQR transition in $CeAl_2$, as obtained by the frequency-swept pulsed spectroscopy described in Sec. II. The important features are a temperature-independent linewidth of 12(2) kHz above T_N, a rapid increase of $\Delta\nu$ just below T_N, and a low-temperature value of 90(10) kHz. This behavior is expected qualitatively from a distribution of hyperfine fields induced by inequivalent Al sites and the modulated AF structure, but the low-temperature linewidth is anomalously small as discussed in Sec. IV.

The error bars in Fig. 1 indicate statistical error only; the bandwidth limitations of the pulsed spectrometer may cause additional inaccuracy in $\Delta\nu$ due to amplitude reduction and phase shift of signal contributions from the "wings" of the NQR line. However the fact that the relative number N_{rel} of observed nuclei, measured as described below, is practically the same at 1.5 and 4.2 K indicates that the linewidths measured at these temperatures are fairly

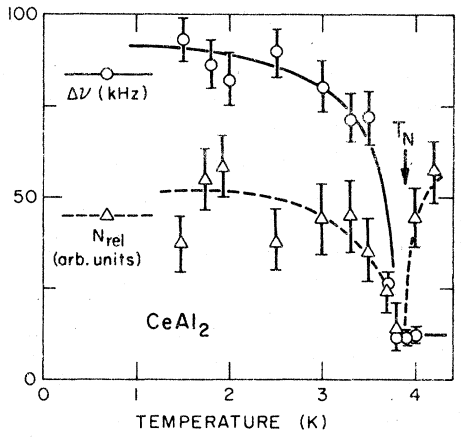

FIG. 1. Half-width-half-maximum ^{27}Al NQR linewidths $\Delta\nu$ (circles) and relative number of observed nuclei N_{rel} (triangles) in the antiferromagnetic state of $CeAl_2$. The observed nuclei are about as numerous at 1.5 K as at 4.2 K, so that spectrometer bandwidth limitations apparently do not narrow the NQR line appreciably.

reliable.

More faithful reproductions of resonance line shapes in the AF state were obtained from field-swept NMR spin-echo spectra as shown in Fig. 2. Here bandwidth limitations are less important, since the spectrometer frequency is fixed at the center of the band. But other broadening mechanisms, principally quadrupolar powder-pattern broadening, anisotropy in the paramagnetic shift, and demagnetization broadening due to distributions of powder grain shapes, are convoluted with the AF-state hf field distribution. The unknown form of demagnetization broadening, in particulaf, makes deconvolution of the NMR line shape impractical, and these spectra are presented principally to demonstrate that the order of magnitude of the AF-state distribution width is the same as obtained in zero-field NQR. No appreciable dependence of the additional broadening on applied field was observed between 6 and 12 kOe.

Linewidth measurements are reliable indicators of hf field distributions only if all nuclei in the sample contribute to the observed resonance. The intensity of the NQR spin-echo signal was measured to obtain the relative number of contributing nuclei, N_{rel}, which is proportional to the product of the signal intensity and the temperature. This quantity is also plotted in Fig. 1, where it is seen that N_{rel} is sensibly the same at 1.5 as at 4.2 K. The dip in N_{rel} in the vicinity of T_N is related to a rapid increase in spin-echo decay rate $1/T_2$ associated with the transition; this increase is not well understood, since no such increase was observed in the longitudinal relaxation rate $1/T_1$ (see below).

Relaxation recovery data were fitted to a two-

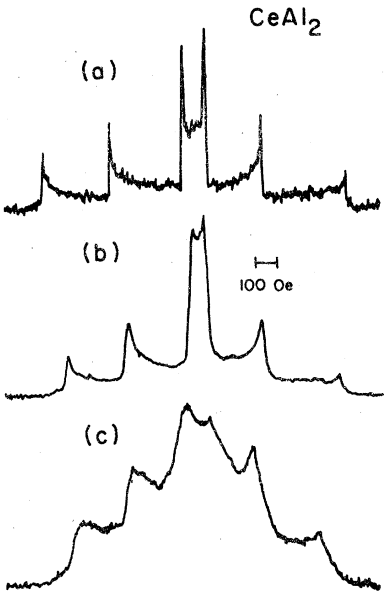

FIG. 2. Field-swept pulsed NMR spectra at an applied field of 6 kOe and (a) 295 K; (b) 4.2 K; and (c) 3 K. The reduction in central transition width between (a) and (b) is due to an anisotropic shift contribution. Demagnetization broadening is also visible in (b). Considerable additional broadening can be seen in (c) in the antiferromagnetic state.

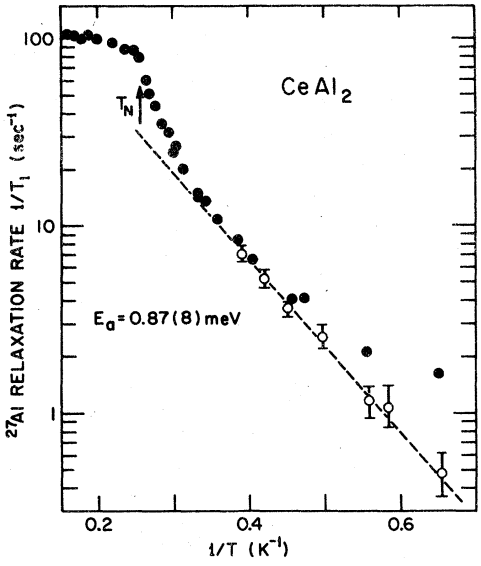

FIG. 3. ^{27}Al spin-lattice relaxation rate $1/T_1$ vs inverse temperature $1/T$ in the antiferromagnetic state of $CeAl_2$. Filled circles: fits to the entire nuclear magnetization recovery. Open circles: fits to the long-time recovery. The latter are consistent with a gap for activation comparable to that found by inelastic neutron scattering (Ref. 6).

exponential expression of the form[22]

$$S(t)-S(\infty)=A_1e^{-3t/T_1}+A_2e^{-10t/T_1}\ , \qquad (2)$$

where $S(t)$ is the observed NQR echo amplitude signal at time t after initial saturation and T_1 is the usual longitudinal spin-lattice relaxation time. The parameters A_1, A_2, and $1/T_1$ were varied for best fit. Above about 2.5 K the quality of the fits was good, as judged from values of the statistic χ^2. Below 2.5 K the quality deteriorated: the recovery of the NQR signal to equilibrium was initially more rapid than consistent with Eq. (2). Incomplete saturation of the observed NQR transition would alter the fit values of A_1 and A_2, but should not diminish the goodness of fit.

We interpret this observation as resulting from the onset of spatially inhomogeneous spin-lattice relaxation at lower temperatures in the AF state. Although the experimental signal-to-noise ratio was not good enough to permit deconvolution of the observed recovery data to obtain the distribution of relaxation rates, information on the distribution was obtained by fitting subsets of data for which points at early times were deleted. The remaining long-time points were more accurately fitted by a curve of the form of Eq. (2), with a relaxation rate appropriate to the most slowly relaxing nuclei. The (poor) fits to the entire relaxation curves (including early-time data) yield relaxation rates which represent weighted averages over the entire distribution. These results are given in Fig. 3.

B. Paramagnetic state

The dependences of the isotropic paramagnetic shift K_i on the temperature and the bulk susceptibility χ are given in Fig. 4. This plot is motivated by the usual expression[19]

$$K_i=(H_{\rm hf}/N\mu_B)\chi \qquad (3)$$

for the relation between K_i and the molar susceptibility χ. Here $H_{\rm hf}$ is the static hyperfine field, N is Avogadro's number, and μ_B is the Bohr magneton. If a single mechanism dominates the temperature dependence of both the susceptibility and the shift, a plot of K_i vs χ will yield a straight line, as has been found for numerous rare-earth intermetallic compounds.[19] It can be seen in Fig. 4 that although a straight-line relationship is obtained above about 50 K, below this temperature the shift is larger than would be predicted from linear extrapolation of the high-temperature data.

The shape of the cw derivative spectra also permitted the extraction of values of the anisotropic shift K_a and the quadrupolar coupling constant e^2qQ/h.[16,19] A rapid increase in K_a is observed below 50 K, in the same temperature region in which

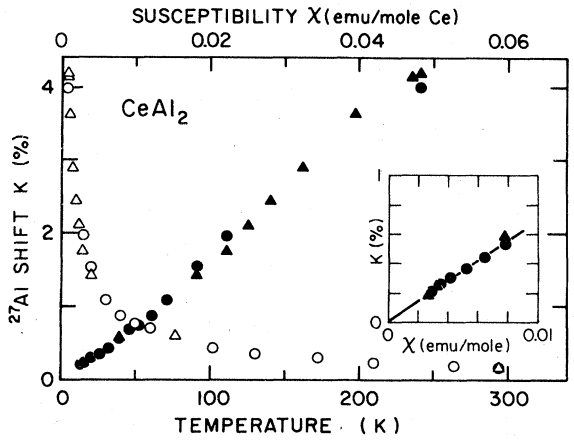

FIG. 4. Dependence of the ^{27}Al isotropic paramagnetic shift K_i on temperature T and bulk susceptibility χ in the paramagnetic state of $CeAl_2$. Open symbols: K_i vs T. Filled symbols: K_i vs χ. Circles: NMR cw derivative spectra. Triangles: pulsed NMR spin-echo spectra.

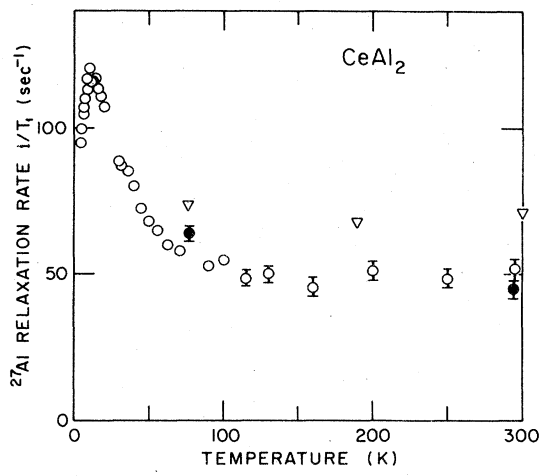

FIG. 6. Temperature dependence of the ^{27}Al spin-lattice relaxation rate $1/T_1$ in the paramagnetic state of $CeAl_2$. Open circles: NQR data (see text). Filled circles: NMR data. Triangles: data of Ref. 14.

K_i deviates from its high-temperature behavior, as shown in Fig. 5(a). The variation of e^2qQ/h with temperature, obtained from both first- and second-order splittings of NMR spectra as well as directly from NQR, is given in Fig. 5(b). The values obtained from second-order splittings are a few percent smaller than those obtained from the other techniques; this may be due to inaccuracies in the method of compensating for finite width of the broadened powder-pattern singularities.[16]

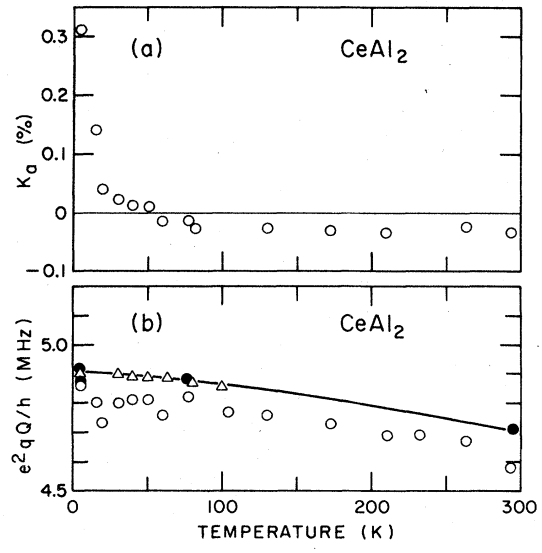

FIG. 5. (a) Temperature dependence of the anisotropic paramagnetic shift K_a. (b) Temperature dependence of the quadrupolar coupling constant e^2qQ/h. Open circles: data from the $\frac{1}{2} \leftrightarrow -\frac{1}{2}$ central NMR transition. Filled circles: data from quadrupolar NMR satellites. Triangles: data from zero-field NQR. Curve: theoretical temperature dependence (see Sec. V A).

The temperature dependence of the ^{27}Al spin-lattice relaxation rate $1/T_1$ in the PM state is shown in Fig. 6. The rate peaks at about 10 K after an increase from the value at T_N. There is no evidence for anomalous behavior near T_N (see also Fig. 3). Between 10 and 100 K the rate decreases by a factor of about 2.5, and then remains constant between 100 and 300 K. Most of these data were obtained using NQR, although NMR values at 77 and 295 K are also shown. Considerable disagreement with earlier measurements[14] is found.

IV. DISCUSSION: ANTIFERROMAGNETIC STATE

A. Line shapes

The onset of a large NQR linewidth below T_N (Fig. 1) is expected, due to the buildup of a static hf field as the Ce spins freeze into particular directions and magnitudes in the ordered state. An exact description of this process is very difficult, since the form of the transferred hf coupling is not well known. In addition, the hf field at a given nucleus is a lattice sum of contributions from Ce neighbors, which must be evaluated for any particular configuration of Ce spin directions and moment magnitudes.

Insofar as the modulated-moment structure possesses one or more modulation wavelengths incommensurate with the crystal lattice, the nuclei will

not experience discrete values of hf fields, but rather a distribution over all allowed values. The existence of line broadening rather than a shift is therefore reasonable. (Any NQR shift was a small fraction of the linewidth.)

The most striking features of the AF-state linewidth is its magnitude. From paramagnetic-state shift measurements, described in Secs. III and V, a value of ~ 5 kOe/μ_B is obtained for the transferred hf field. This is then by definition the local field experienced by a ^{27}Al nucleus per Bohr magneton induced on each (equivalent) Ce ion by the applied field in the PM state. A fit to AF state neutron Bragg intensity measurements,[8] based on a particular assumed modulation configuration, indicates an average moment somewhat less than the Γ_7-state value of 0.71 μ_B. If each Ce moment contributed the same hf field in the AF state as in the PM state, one would expect a hf field distribution with a width of the order of ~ 3 kOe. The observed low-temperature width (in field units $\Delta H = 2\pi\Delta\nu/\gamma$, where γ is the ^{27}Al gyromagnetic ratio) of 81(9) Oe is more than an order of magnitude smaller.

Measurements of the nuclear hyperfine specific heat in $CeAl_2$ for $T < 50$ mK indicate an average hf field in the AF state which is reduced by a factor of 3 from the paramagnetic-state value.[23] This is still an order of magnitude larger than the NQR width, so that a discrepancy exists between NQR and specific-heat measurements.

An effect of lattice symmetry combined with AF order can reduce the hf field summed over Ce lattice sites. To see this effect in a simple example, consider a nucleus equidistant between two antiparallel moments. Assuming an isotropic hf interaction, the resultant hf field at the nucleus is zero.

The situation in $CeAl_2$ is much more complicated than in this example. The Ce ions form a diamond lattice in the $C15$ structure, and the Al ions occupy the interstices of the diamond structure as tetrahedra with symmetry axes in [111] directions. In the paramagnetic state the Ce polarization induced by the applied field is spatially uniform, and all ^{27}Al sites are equivalent. The situation in the AF state depends in detail on the kind of AF order. If, as suggested by Barbara *et al.*,[8] Ce spins are aligned parallel within (111) planes and antiparallel between adjacent (111) planes, then in the absence of moment modulation[8] one of the four ^{27}Al sites in a tetrahedron satisfies the symmetry condition described in the preceeding paragraph: this is the site whose threefold rotation symmetry axis lies in the AF [111] direction.

Since the pairwise hf field $\vec{H}_{hf}(\vec{r}_{ij})$ is not well known experimentally and is extremely hard to obtain theoretically,[24] we have used a simple RKKY (Ruderman-Kittel-Kasuya-Yosida) model to estimate the order of magnitude of expected hf fields for various spin configurations. This yields a pairwise hf field of the form

$$\vec{H}_{hf}(\vec{r}_{ij}) \propto \vec{S}_i F(2k_F r_{ij}) \ , \tag{4}$$

where

$$F(x) = (x\cos x - \sin x)/x^4 \ , \tag{5}$$

$\vec{S}_i$ is the spin at the ith Ce site, k_F is the Fermi wave vector of the assumed free-electron conduction band, and r_{ij} is the distance between Ce spin i and ^{27}Al nucleus j. This approach has been used previously by Buschow and co-workers,[24,25] who also calculated lattice sums between rare-earth sites to obtain paramagnetic Curie-Weiss temperatures. It is taken here as the simplest model for the hf coupling. Band-structure effects are partially taken into account by treating k_F as a free parameter.

Lattice sums in the $C15$ structure were carried out over up to 125 cubic unit cells for three cases: (a) a uniform Ce-spin polarization (paramagnetic state); (b) an unmodulated AF structure of [111]-direction ferromagnetic planes; and (c) an AF structure with moment modulation in the $[1\bar{1}0]$ direction.[8] In case (c) the modulation wavelength was set at 4 cubic unit cell face diagonals for ease of calculation; the incommensurate wavelength for the structure of Barbara *et al.*[8] is not far from this value. For case (b) the hf field vanishes at the symmetric ^{27}Al site.

Figure 7(a) gives the RKKY lattice sum $\sum_i S_i F(2k_f R_{ij})$ as a function of reduced Fermi vector k_F/k_{F0}, where k_{F0} is the free-electron value calculated

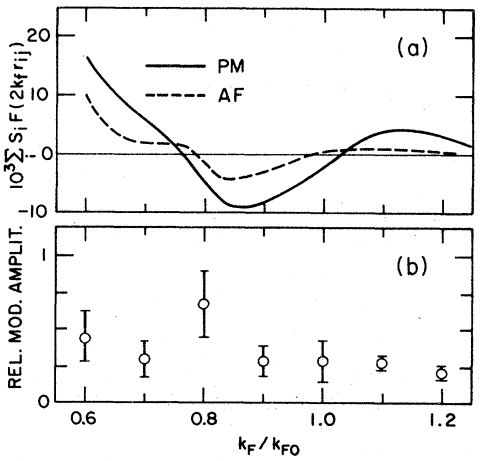

FIG. 7. (a) RKKY lattice sums (see text) over Ce sites i with an Al site j at the origin, in paramagnetic and unmodulated antiferromagnetic configurations of Ce ions. The reduced Fermi wave vector k_F/k_{F0} is varied to simulate non-free electron band structures. (b) Amplitudes of lattice sums for the "single-q" modulated antiferromagnetic structure described in the text, relative to the paramagnetic-state lattice sum [Fig. 7(a)]. The bars give ranges of values obtained for the four nonequivalent ^{27}Al sites.

on the basis of three conduction electrons per atom. The PM-state values [case (a)] agree well with the results of Buschow *et al.*[25] The AF case was calculated using $S_i = \pm 1$ for the two sublattices.

For case (c) the resultant hf field is a sinusoidal function of the phase of the moment modulation. The amplitude of this modulation, relative to the PM-state hf field, is shown in Fig. 7(b). The general trend indicates a reduction of the hf field amplitude by about 70% due to the combined effects of modulation and AF order. This reduction is insufficient to account for the reduction of a factor of about 30 observed in the NQR linewidth.

The fact that the number of nuclei in small hf field is larger than predicted from a single-q modulated structure may originate in the existence of more than one direction of modulation, as proposed by Shapiro *et al.*[10] To demonstrate this point, a simple model for the modulated sublattice magnetization distribution in space of the form

$$M(\vec{r}) = M_0 \prod_{i=1}^{d} \sin x_i \qquad (6)$$

has been investigated numerically. Here d is the number of assumed modulation directions; the wavelength has been taken as equal in all directions for simplicity. [We note that the presence of an appreciable fraction of sample volume in regions of low $M(\vec{r})$ is dependent upon commensurability in all d directions and also upon the relative phases; the nodes of all the $\sin x_i$ must be coincident.] Figure 8 gives the probability distribution $P(M)$ for $M(\vec{r})$ given by Eq. (6) and $d = 1$, 2, and 3. It can be seen that the distribution narrows considerably as d is increased. A combination of this effect and the structural reduction of the hf field [Fig. 7(b)] is suggested as the origin of the observed narrow NQR line.

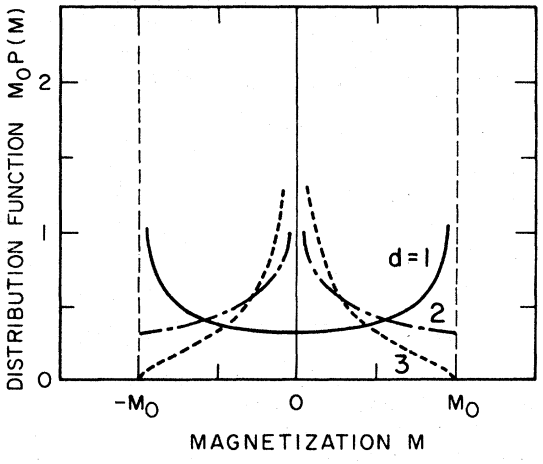

FIG. 8. Model distribution functions for the sublattice magnetization density in simple modulated antiferromagnetic structure given by Eq. (6) of the text. Solid curve: one modulation direction. Dash-dot curve: 2 modulation directions. Dashed curve: 3 modulation directions.

It must be stressed, however, that the above model calculations are highly simplified, and that a more realistic form for $F(2k_F R_{ij})$ and for the multiple-q structure would both be required for comparison with experiment. In addition there remains the experimental discrepancy between the present NQR results and the nuclear hf specific-heat data,[23] which is not understood at the present time.

B. Relaxation

The relaxation rate $1/T_1$ in the AF state, given in Fig. 3, exhibits a number of features. The minimum (long-time) values of $1/T_1$ (see Sec. III A) vary approximately exponentially with inverse temperature. If this variation is attributed to activation over an energy gap, the value of the gap is 0.87(8) meV. This is to be compared to a "magnon" inelastic neutron peak between 0.8 and 1.3 meV observed by Loewenhaupt and Steglich.[6] The agreement is good.

The inhomogeneous relaxation observed below 2.5 K, discussed in Sec. III A, indicates the presence of regions in the sample where Ce spin fluctuations relax nuclei more strongly than expected for thermally-activated magnons. This additional relaxation is tentatively attributed to Ce spin fluctuations in regions of the sample near nodes in the moment modulation; i.e., where Kondo coupling to the conduction electrons results in relatively slow spin fluctuations.

Impurity spin fluctuations in the Kondo alloy *Cu*Fe have been extensively studied by host ^{63}Cu NMR and by quasielastic neutron scattering.[11] A simple expression is obtained for the order of magnitude of the expected NMR relaxation rate at low temperatures $T \ll T_K$, under the assumptions that (a) the static susceptibility χ of the Kondo impurity is of the order of $\mu_B^2/k_B T_K$, and (b) the spin fluctuation time τ is of the order of $\hbar/k_B T_K$. Standard relaxation theory[26] then yields

$$1/T_1 \simeq (\gamma_n H_{\rm hf}/\mu_B)^2 k_B T \chi \tau/\hbar \simeq \hbar(\gamma_n H_{\rm hf})^2 T/k_B T_K^2 \ , \qquad (7)$$

where $H_{\rm hf}$ is the hf coupling field.

Using the paramagnetic-shift data to estimate $H_{\rm hf} \simeq 5$ kOe, as described in Sec. V, we obtain an estimated fluctuation-induced relaxation rate

$$1/T_1 \simeq 300T(\sec^{-1}) \ , \qquad (8)$$

where $T_K \simeq 5$ K has been obtained from a number of studies.[9] Equation (8) overestimates the observed "average" low-temperature rate (Fig. 3) by more than two orders of magnitude.

Several effects may play a role in removing this

discrepancy, although the understanding of the low-temperature state of $CeAl_2$ is not sufficiently advanced to discriminate between them. First, spatial correlation between hf field contributions from various Ce neighbors of a given nucleus can render a simple estimate of H_{hf} from paramagnetic shifts inadequate for purposes of estimating relaxation rates.[14] In particular, the absence of correlation between neighboring fluctuations would tend to reduce $1/T_1$ by a factor n_{eff}, which can be interpreted as an effective number of Ce neighbors to a ^{27}Al nucleus as discussed in Sec. V. In the PM state at high temperatures $n_{eff} \sim 10$ is obtained. Although this number is unlikely to characterize the AF state, some of the discrepancy may be accounted for by (partially) uncorrelated Kondo fluctuations of neighboring Ce ions.

The remaining disagreement may be related to the crudeness of Eq. (7), but in addition it is rather likely that spin-spin couplings between Ce ions in "Kondo" states at the nodes of the modulated structure act either to reduce the amplitudes or to increase the rates of local spin fluctuations. A theoretical investigation of the dynamics of Kondo spins in the presence of spin-spin interactions would be very useful in elucidating this point.

The NMR relaxation data near T_N give no indication of critical behavior at the transition. This is rather surprising, in view of the lambda anomaly in the specific heat[27] and the inflection point in the susceptibility[18] at T_N, both of which indicate an extended critical region. It is possible that the low-frequency fluctuations effective for nuclear relaxation are suppressed by local Kondo spin fluctuations. Again, more detailed theoretical guidance would be useful to understand this result.

V. DISCUSSION: PARAMAGNETIC STATE

A. Absorption spectra

The most important feature of the isotropic shift measurements is the change of slope in K_i versus the susceptibility (Fig. 4). This indicates a temperature dependence of the hf coupling. Such a dependence is expected if the hf field is anisotropic, since then the restricted symmetry of the Γ_7 ground-state wave function will cause it to couple differently to neighboring nuclei than the Γ_8 state.[12]

A simple model for this effect assigns a phenomenological hf coupling field H_m to the mth CEF-split state, and takes the contribution of the mth state to the total shift to be proportional to the product of H_m and the susceptibility contribution χ_m. Since the temperature dependences of the χ_m are well known,[28] an expression for the effective time-average hf field $\langle H_{hf} \rangle$, defined by

$$K_i(T) = \langle H_{hf}(T) \rangle \chi(T)/N\mu_B \tag{9}$$

is readily found:

$$\langle H_{hf} \rangle = \sum_m H_m P_m(T) \ , \tag{10}$$

where

$$P_m = \sum_n Q_{mn} \Big/ \sum_{mn} Q_{mn} \tag{11}$$

and

$$Q_{mn} = |m_{mn}|^2 e^{-\beta E_n}(1 - e^{-\beta \Delta_{mn}})/\Delta_{mn} \ , \tag{12}$$

with

$$|m_{mn}|^2 = |\langle n | g\mu_B J_z | m \rangle|^2 \ . \tag{13}$$

Here $\beta = 1/k_B T$ is inverse temperature, E_n is the energy of CEF states n, Δ_{mn} is the energy difference between states m and n, and the sums are over all states.[28]

This leads to the temperature dependence of $\langle H_{hf} \rangle$ given in Fig. 9, with the CEF splitting set[6] at 100 K and the values of H_7 and H_8 adjusted to fit the low- and high-temperature data, respectively. The experimental points are obtained from Eq. (9) after subtraction of the high-temperature intercept $K_{i0} = 0.01(2)\%$ (Fig. 4). The agreement with the theoretical form is quite satisfactory.

We note that $H_7 > H_8$ for the fit. This result is opposite to that found in some other Ce-based systems,[12] and cannot be explained by the effective CEF-state-dependent exchange constant $J_{MM'}$ derived by Cornut and Coqblin.[29] In this theory $\langle H_{hf} \rangle$ is smaller for the ground CEF state than for excited states due to an energy denominator in the modified

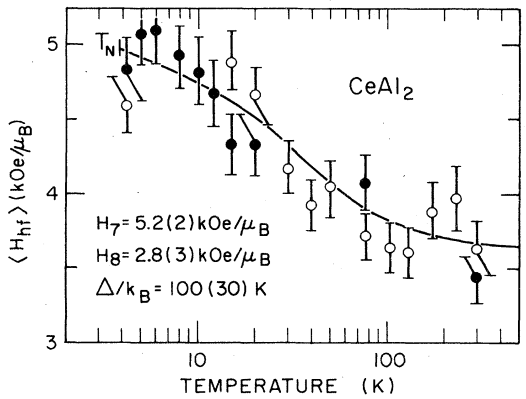

FIG. 9. Temperature dependence of the average ^{27}Al hyperfine field $\langle H_{hf} \rangle$ in the paramagnetic state of $CeAl_2$. Open circles: NMR cw derivative spectra. Filled circles: pulsed NMR spin-echo spectra. Solid line: model calculation [text, Eqs. (10)–(13)], with parameter values indicated.

Schrieffer-Wolff-Coqblin expression for $J_{MM'}$.[29] It appears that some other coupling mechanism, such as polarization of Ce $5d$ virtual bound states,[24] may be involved. Such interactions may also play a role in Ce spin-spin couplings, and must be better understood to obtain a clearer picture of the antiferromagnetic phase transition.

The anisotropic shift K_a is partially accounted for by dipolar interactions between Ce ions and ^{27}Al nuclei, as reported previously.[16] Dipolar coupling provides all the anisotropic shift at 300 K to within experimental error, and gives a temperature variation opposite to that observed [Fig. 5(a)]. The temperature variation of the nondipolar contribution, obtained by subtracting the calculated dipolar component from the observed values of K_a, (Ref. 16) is similar to that of the static hf field $\langle H_{hf} \rangle$ relative to its high-temperature value, and is very likely due to the same anisotropic mechanism. This point is corroborated by the fact that the low-temperature PM-state values of K_a relative to K_i (~ 0.2) are about two orders of magnitude greater than the relative anisotropy in the susceptibility.[30]

The electric field gradient $q(T)$ in simple metals is found to have a temperature dependence of the form

$$q(T) = q(0)(1 - aT^b) \ , \tag{14}$$

where $b \simeq 1.5$ is a number of cases.[31] The curve in Fig. 5(b) is of this form, and is in good agreement with the more accurate data. The $T^{3/2}$ temperature dependence has been attributed to the interaction between conduction electrons and phonons in the metal.[31] The measured ratio $q(300\ \text{K})/q(0) \simeq 0.96$ for $CeAl_2$ is somewhat larger than for nontransition metals. The absence of additional temperature dependence, particularly below 100 K, indicates that the Ce $4f$ charge contribution to $q(T)$ is either (a) very small or (b) nearly the same in the Γ_7 and Γ_8 CEF states. The former possibility is likely if conduction states derived from Ce $5d$ wave functions efficiently screen the $4f$ charge.

B. Spin-lattice relaxation

The mechanisms which lead to the temperature dependence of spin-lattice relaxation rates in the paramagnetic state have been reviewed recently.[32] The processes of interest for $CeAl_2$ include (1) possible temperature dependences of the Ce-ion spin fluctuation rates (critical slowing down, temperature-dependent conduction-electron scattering[13]), and the onset at lower temperatures of short-range spatial correlations (short-range order) in the Ce spin system. This latter phenomenon is manifested only because the probe ^{27}Al nuclei sense hyperfine fields from several Ce neighbors; the ^{27}Al relaxation time is therefore sensitive to correlations between stochastic motions of Ce neighbors as well as to the single-Ce spin fluctuation time.

A convenient definition of the latter quantity for NMR purposes is given by

$$\tau = \frac{\sum_q \chi''(q, \omega_n)/\omega_n}{N\chi'(0,0)} \ , \tag{15}$$

where $\chi(q, \omega) = \chi'(q, \omega) + i\chi''(q, \omega)$ is the complex Ce dynamic spin susceptibility and N the number of Ce ions. The sum is over spatial fluctuation modes with wave vectors q. The frequency dependence of τ is slight if the nuclear resonance frequency ω_n is much less than characteristic fluctuation rates, i.e., if $\omega_n \tau \ll 1$.

If the probe nuclei are each coupled to only one $4f$ ion in a hypothetical compound, then it is easy to show[33] that

$$\chi_b / K_i^2 T_1 T = 2N\gamma_n^2 k_B \tau \ , \tag{16}$$

where χ_b is the bulk $4f$ susceptibility. In the more general case (appropriate to $CeAl_2$) the form of Eq. (16) still holds,[33] with τ replaced by

$$\tau_{eff} = \frac{\sum_q |H_{hf}^{(q)}|^2 \chi''(q, \omega_n)/\omega_n}{N[H_{hf}^{(0)}]^2 \chi'(0,0)} \ . \tag{17}$$

Here $H_{hf}^{(q)}$ is the spatial Fourier transform of the transferred hf field $H_{hf}(r)$ between a Ce ion and a ^{27}Al nucleus separated a distance r. If a given nucleus is coupled to only one ion $H_{hf}^{(q)}$ is independent of q, and Eq. (17) reduces to Eq. (15).

In the absence of correlation between Ce spin fluctuations the dynamic susceptibility is independent of wave vector, so that

$$\tau_{eff} = C(H_{hf})\tau \ , \tag{18}$$

where

$$C(H_{hf}) = \sum_q |H_{hf}^{(q)}|^2 / N[H_{hf}^{(0)}]^2 = \sum_r H_{hf}^2(r) \Big/ \left[\sum_r H_{hf}(r)\right]^2 \tag{19}$$

is a prefactor describing the hyperfine coupling in the crystal lattice. We can interpret $C(H_{hf})$ as the inverse of an effective NMR Ce coordination number n_{eff}, since if n_{eff} neighbors each give equal contributions to the field at the nucleus it is easy to show that

$$C(H_{hf}) = 1/n_{eff} \ . \tag{20}$$

Figure 10 gives the temperature dependence of τ_{eff}^{-1} obtained from the NMR data, measured bulk susceptibilities, and Eq. (16). If only these data were available, one would conclude that above 100 K the fluctuation rate is approximately constant and that below

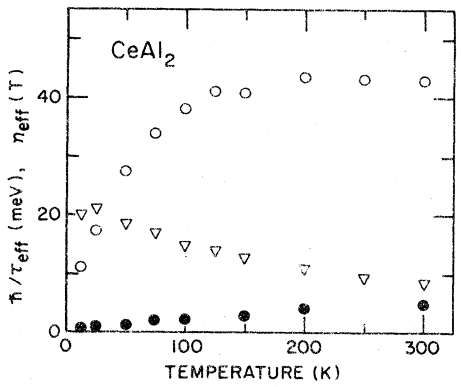

FIG. 10. Temperature dependences of effective fluctuations rates $1/\tau_{\rm eff}$ and the ratio $n_{\rm eff}(T)=\tau/\tau_{\rm eff}$ in the paramagnetic state of $CeAl_2$. Open circles: $\hbar/\tau_{\rm eff}$ from NMR and susceptibility data [Eq. (17)]. Filled circles: $\hbar/\tau_{\rm eff}$ from neutron quasielastic scattering (Ref. 13). Triangles: $n_{\rm eff}(T)$, assuming $\tau=\tau_{\rm eff}$ (neutron).

100 K the onset of ferromagnetic short-range order[14] increases $1/T_1$ (thereby decreasing $1/\tau_{\rm eff}$) without directly affecting the hf field. Such a picture would be consistent with the results of momentum-resolved neutron scattering measurements,[9] which also indicated initially ferromagnetic correlations below about 80 K.

But quasielastic neutron-scattering studies of the dynamic susceptibility have also been carried out in $CeAl_2$.[13] The quasielastic peak linewidths observed in those experiments are also plotted in Fig. 10; they are considerably smaller than the NMR values of $1/\tau_{\rm eff}$. At high temperatures the prefactor $C(H_{\rm hf})$ in Eq. (18), which is valid for no short-range order,[14] may be significantly less than unity, so that the expected ratio of the experimental NMR and neutron fluctuation rates is biased in the observed direction. If no correlation is assumed to be present at 300 K, then a value of the NMR coordination number $n_{\rm eff}=9(2)$ is obtained, to be compared with the crystallographic number of 6 Ce nearest neighbors to an Al site. This result is reasonable.

The additional information available from the neutron measurements can be used if it is assumed that the quasielastic linewidth is in fact equal to the inverse of τ defined by Eq. (15). The temperature variation of the quantity

$$n_{\rm eff}(T)=\tau/\tau_{\rm eff}\ , \tag{21}$$

(which no longer can be interpreted as a coordination number) then reflects the nature (ferromagnetic or antiferromagnetic) of the short-range order. This is due to the bias given to $n_{\rm eff}(T)$ by the $H_{\rm hf}^{(q)}$ appearing in Eq. (17): if for reasons of symmetry $H_{\rm hf}^{(q)}$ is small or vanishes for q appropriate to antiferromagnetic fluctuations, for example, one will expect $n_{\rm eff}(T)$ to increase with decreasing temperature. If on the contrary ferromagnetic correlations set in, then $n_{\rm eff}(T)$ should approach unity as the Ce spin system fluctuates coherently as a single "giant" spin.

The temperature dependence of $n_{\rm eff}(T)$ is also plotted in Fig. 10, where an increase with decreasing temperature can be seen. Thus this analysis leads to the conclusion that short-range order is antiferromagnetic, which is opposite to the above analysis of the NMR data alone.

The possibility remains that since neutron scattering and NMR investigations are actually probing different parts of the fluctuation spectrum, the results of the two techniques should not be compared. In fact, the rather large temperature dependence of the neutron quasielastic linewidth is surprising at temperatures more than an order of magnitude above T_N, if the linewidth were dominated by spin-spin interactions; these should yield temperature-independent fluctuations in the high-temperature limit.[14] The neutron results have been interpreted as resulting from conduction-electron scattering (the Korringa mechanism),[13] but this does not answer the question of why the spin-spin interactions are ineffective in influencing the fluctuation spectrum. Indeed, if only Korringa scattering (possibly modified by the Kondo effect[11]) were involved, Ce fluctuations would be uncorrelated and the neutron and NMR fluctuation rates should track each other's temperature dependence to within a constant factor $1/n_{\rm eff}$ [Eq. (17)]. This is certainly not observed, and we interpret the temperature dependence of the ratio of the fluctuation rates as an indication that either (a) correlations are important, and attribution of the fluctuations to the Korringa mechanism for fluctuations is only partially correct, or (b) neutron and NMR measurements probe different mechanisms, on account of their vastly different characteristic frequencies (10^9 $\sec^{-1}$ for NMR; 10^{13} $\sec^{-1}$ for neutrons).

It would be very useful to have neutron data for low momentum transfers, as direct probes of the nature of the spatial correlations.

VI. CONCLUSIONS

Nuclear resonance experiments in $CeAl_2$ have yielded information on spin configurations and low-lying fluctuations in the antiferromagnetic ground state, and on Ce spin correlations and crystal-field effects in the transferred hyperfine field in the paramagnetic high-temperature state. In the antiferromagnetic state a serious discrepancy exists between hyperfine field values obtained from zero-field NQR spectra at 1.5 K and from nuclear hyperfine specific-heat measurements below 50 mK.[23] The latter exper-

iments yield a hyperfine-field value three times smaller than that obtained by NMR in the paramagnetic state; such an effect was in fact obtained using a "single-q" model for Ce moment modulation in Sec. IV, and is a consequence of (average) Al site symmetry with respect to the modulated structure. But the NQR linewidths at 1.5 K are narrower by an order of magnitude than such an effect can explain. We tentatively identify this result with the presence of coherent moment modulation in several directions (the "multiple-q" structure), in which cospatial nodes provide an appreciable fraction of the specimen for which the local hyperfine field is anomalously small. The discrepancy with the specific-heat results is not understood; a change of magnetic structure between 50 mK and 1.5 K is one hypothetical cause which, however, finds no justification in other experiments.[9]

The onset of inhomogeneous relaxation below $\sim 0.65 T_N$ is attributed to the same modulated structure. Regions of rapid nuclear relaxation (high low-frequency noise power) are those for which single-ion Kondo condensation[3] has reduced the frequencies of the low-lying excitations. Regions of large Ce magnetization density are characterized by an energy gap for excitations typical of antiferromagnetic magnons. A similar "softening" of the mode structure by the Kondo effect has been invoked by Walker and Walstedt[34] to explain the low-temperature behavior of the magnetic specific heat in spin-glass *Au*Fe, which is another system for which competition between the Kondo effect and magnetic ordering should exist.

The temperature dependence of the time-averaged hyperfine field in the paramagnetic state is given a natural explanation if the hyperfine coupling differs between crystal-field split Ce ionic states; i.e., the coupling is anisotropic. This conclusion is also consistent with the rapid onset of an appreciable anisotropic shift (Fig. 5) as the excited crystal-field level is depopulated below 100 K.

The relaxation-rate increase below 100 K might at first sight be attributed to the increase in the hyperfine coupling, but the increase is considerably larger than can be so explained. The effective NMR fluctuation rate $\tau_{\rm eff}^{-1}$ is normalized to remove the direct effect of a temperature-dependent coupling, and nevertheless exhibits a strong decrease below 100 K (Fig. 10). This dependence is opposite in direction to that predicted by Sugawara[15] on the basis of crystal-field effects on the fluctuation spectrum, and its cause must be sought in an understanding of the temperature dependence of the low-frequency fluctuation power per Ce spin, or the effect of spatial correlation of Ce spins on the behavior of the hyperfine field, or both of these considerations.

The present investigation, in contrast to a previous study of NMR and neutron-scattering estimates of fluctuation rates in the intermediate-valent compound YbCuAl,[33,35] yields a wide discrepancy between NMR and neutron fluctuation rates. Although part of this discrepancy is probably due to symmetry effects in the hyperfine coupling for NMR, the temperature dependences of the two measured fluctuation rates are not easily understood in a common theoretical picture. In particular, it is hard to understand the NMR data if the Ce fluctuations are dominated by conduction-electron Korringa scattering, as suggested by the neutron results.[13] Clearly more work is required to understand dynamic processes in this complex system.

ACKNOWLEDGMENTS

We are grateful to F. R. de Boer for help with sample preparation, J. M. Lawrence for carrying out susceptibility measurements, and to T. Keller and J. Mullin for assistance with the experiments. One of us (D. E. M.) wishes to thank P. F. de Châtel, J. Bijvoet, and the Natuurkundig Laboratorium, University of Amsterdam, Netherlands, for their hospitality during a visit when part of this work was carried out. We are indebted to all of the above as well as M. Croft, M. Loewenhaupt, R. D. Parks, and F. Steglich for useful discussions. This work was supported in part by the National Science Foundation under Grant No. DMR-7810301, and in part by the University of California, Riverside, Committee on Research.

[1]F. Steglich, Z. Phys. B 23, 331 (1976).

[2]See the numerous articles on $CeAl_2$ and related materials in *Valence Instabilities and Related Narrow-Band Phenomena,* edited by R. D. Parks (Plenum, New York, 1977).

[3]R. Jullien, J. N. Fields, and S. Doniach, Phys. Rev. B 16, 4889 (1978).

[4]K. H. J. Buschow and H. J. van Daal, Phys. Rev. Lett. 23, 408 (1969).

[5]E. Walker, H.-G. Purwins, M. Landolt, and F. Hulliger, J. Less-Common Met. 33, 203 (1973), and references therein.

[6]M. Loewenhaupt and F. Steglich, Physica (Utrecht) 86–88B, 187 (1977).

[7]M. Loewenhaupt and F. Steglich, in *Crystal Field Effects in Metals and Alloys,* edited by A. Furrer (Plenum, New York, 1977), p. 198.

[8]B. Barbara, J. X. Boucherle, J. L. Buevoz, M. F. Rossignol, and J. Schweizer, Solid State Commun. 24, 481 (1977); 29, 810 (E) (1979).
[9]F. Steglich, C. D. Bredl, M. Loewenhaupt, and K. D. Schotte, J. Phys. (Paris) 40, C5-301 (1979).
[10]S. M. Shapiro, E. Gurewitz, R. D. Parks, and L. C. Kupferberg, Phys. Rev. Lett. 43, 1748 (1979).
[11]M. Loewenhaupt and W. Just, Phys. Lett. 53A, 305 (1975); H. Alloul, Physica (Utrecht) 86–88B, 449 (1977).
[12]S. M. Myers and A. Narath, Solid State Commun. 12, 83 (1973); D. M. Follstaedt, W. J. Meyer, and A. Narath, Physica (Utrecht) 86–88B, 507 (1977).
[13]M. Loewenhaupt (unpublished).
[14]B. G. Silbernagel, V. Jaccarino, P. Pincus, and J. H. Wernick, Phys. Rev. Lett. 20, 1091 (1968); C. Sherer, J. E. Gulley, D. Hone, and V. Jaccarino, Rev. Bras. Fis. 4, 299 (1974).
[15]K. Sugawara, J. Phys. Soc. Jpn. 42, 1161 (1977); 44, 1491 (1978).
[16]D. E. MacLaughlin and R. R. Hewitt, J. Appl. Phys. 49, 2121 (1978).
[17]D. E. MacLaughlin, J. Magn. Magn. Mater. 17, 695 (1980).
[18]I. Zorić, J. Markovics, L. Kupferberg, M. Croft, and R. D. Parks, in Ref. 2, p. 479.
[19]See G. C. Carter, L. H. Bennett, and D. J. Kahan, Prog. Mater. Sci. 20, 1 (1977) for a review of NMR techniques; also I. D. Weisman, L. J. Swartzendruber, and L. H. Bennett, in *Techniques of Metals Research,* edited by E. Passaglia (Wiley, New York, 1973).
[20]D. E. MacLaughlin and M. Daugherty, Phys. Rev. B 6, 2502 (1972).
[21]A. Narath, Phys. Rev. 162, 320 (1967).
[22]D. E. MacLaughlin, J. D. Williamson, and J. Butterworth, Phys. Rev. B 4, 60 (1971); 5, 241(E) (1972).
[23]H. Armbrüster and F. Steglich, Solid State Commun. 27, 873 (1978).
[24]K. H. J. Buschow, Rep. Prog. Phys. 42, 1373 (1979), and references therein.
[25]K. H. J. Buschow, J. F. Fast, A. M. van Diepen, and H. W. de Wijn, Phys. Status Solidi 24, 715 (1967).
[26]A. Narath, Crit. Rev. Solid State Sci. 3, 1 (1972).
[27]R. W. Hill and J. M. Machado da Silva, Phys. Lett. 30A, 13 (1969).
[28]T. Murao and T. Matsubara, Prog. Theor. Phys. (Kyoto) 18, 215 (1957).
[29]B. Cornut and B. Coqblin, Phys. Rev. B 5, 4541 (1972).
[30]R. W. Cochrane, F. T. Hedgcock, J. O. Ström-Olsen, and G. Williams, J. Magn. Magn. Mater. 7, 137 (1978).
[31]K. Nishiyama and D. Riegel, Hyper. Inter. 4, 490 (1978).
[32]E. Dormann, R. D. Hogg, D. Hone, and V. Jaccarino, Physica (Utrecht) 86–88B, 1183 (1977); R. D. Hogg, Ph.D thesis (University of California, Santa Barbara, 1975) (unpublished).
[33]D. E. MacLaughlin, F. R. de Boer, J. Bijvoet, P. F. de Châtel, and W. C. M. Mattens, J. Appl. Phys. 50, 2094 (1979).
[34]L. R. Walker and R. E. Walstedt (unpublished).
[35]W. C. M. Mattens, F. R. de Boer, A. P. Murani, and G. H. Lander, J. Magn. Magn. Mater. 17, 973 (1980).